Iranian Journal of Medical Physics
Vol. 11, No. 4, Autumn 2014, 294-300
Received: May 4, 2014; Accepted: August 03, 2014

Original Article

Radiation Effects on the On-line Monitoring System of a Hadrontherapy Center

Abdolkazem Ansarinejad[1*], Anna Ferrari[2]

Abstract

Introduction
Today, there is a growing interest in the use of hadrontherapy as an advanced radiotherapy technique. Hadrontherapy is considered a promising tool for cancer treatment, given its high radiobiological effectiveness and high accuracy of dose deposition due to the physical properties of hadrons. However, new radiation modalities of dose delivery and on-line beam monitoring play crucial roles in a successful treatment. In hadrontherapy, through interactions between the primary beam and patient's tissue, secondary neutrons are produced.
Materials and Methods
This study, by using FLUKA Monte Carlo simulations, assessed the level of secondary neutron radiation, produced during patient treatment. In addition, the evaluation included secondary neutron radiation, which was produced while hitting the on-line detectors of beam delivery system by the Italian National Center for Hadrontherapy (CNAO). This study assessed the effects of secondary neutron radiation on an electronics rack (including a data acquisition system, a power supply, and a gas system) and a nozzle, where two monitoring boxes (each one consisting of two or three parallel plate ionization chambers) were installed.
Results
The resulting neutron energy spectra and radiation doses were used to determine the life performance and the probability of damage to these devices. Findings showed that by using carbon ions of 400 MeV/u, the fluence rate of secondary neutrons will be approximately 3.4×10^{10} n/cm^2 in a year.
Conclusion
This value is lower than the experimental threshold, which is responsible for less than 1% of changes in electrical characteristics, and would cause no single event upsets.
Keywords: Neutron Diffraction; Proton Therapy; Radiation Effects; Monte Carlo Method.

1- Physics and Accelarators Research School, Nuclear Science and Technology Research Institute, Tehran, Iran
*Corresponding author: Tel:+982182063236; Fax:+982188221074; E-mail: kazemansar@gmail.com

2- Institute of Nuclear Safety Research, Institute of Radiation Physics, Helmholtz-Zentrum Dresden-Rossendorf (HZDR), Dresden, Germany

1. Introduction

In hadrontherapy, secondary neutrons are produced by interactions between the primary beam, beam transport system, and patient's tissue; in treatment rooms, the interaction between the primary beam and patient's tissue is more dominant.

There has been a growing interest in determining radiation damage to electronic components and detectors, which are essential parts of the monitoring system by the Italian National Center of Oncological Hadrotherapy (CNAO). By using a simplified but realistic description of a treatment room and making conservative assumptions for irradiation was computed the secondary neutron fluence arriving on the nozzle and rack surface (figures 1 & 2). To estimate the effects of these secondry particles, simulations were performed, using FLUKA MONTE Carlo Code [1, 2 and 3].

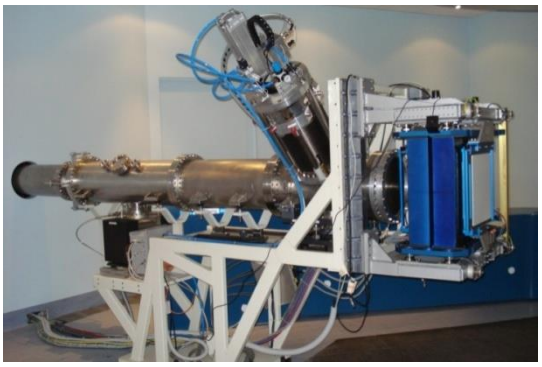

Figure 1. The nozzle with the monitoring system installed in front of the beamline.

Figure 2. The electronics rack containing a data acquisition system, a power supply, and a gas panel.

Afterwards, the estimated values were compared with the results obtained in Large Hadron Collider (LHC) experiment, on electronic devices with metal oxide semiconductor (MOS) and complementary MOS (CMOS) technology, and study of Radiation effects on the Tera-VLSI (Very Large Scale Integration) chip, which is used as the front-end readout of detectors which were installed at the proton therapy center of Paul Scherrer Institute (PSI), Switzerland. The mentioned experiments aimed to study the life performance of these devices and assess the caused damage [4].

The mentioned study described the simulation of neutron radiation produced by carbon ion beams at maximum operational energy of 400 MeV/u. Neutron radiation effects were evaluated on 1) the surface of the nozzle, which consisted of a holding structure and two boxes, each one consisting of two (Box 1) and three (Box 2) parallel plate ionization chambers; and 2) the surface of the electronics rack, where a data acquisition system, a power supply, and a gas distribution system were installed[2].

2. Materials and Methods

2.1. Monte Carlo simulation technique

FLUKA code (version 2008.3c) was used for all simulation stages. FLUKA is one of the few codes available for this sort of calculations. This code can describe heavy ion collisions including the transport of fragments, together with the entire hadronic and electromagnetic cascades (including the evaluation of neutron contribution to thermal energies). Before evaluating the neutron spectra, a general overview of materials and the geometry model for the description of treatment room is provided in the next sections [3, 5].

2.2. Position of the neutron source

The neutron source was located at the isocenter of the treatment room (fig. 3).

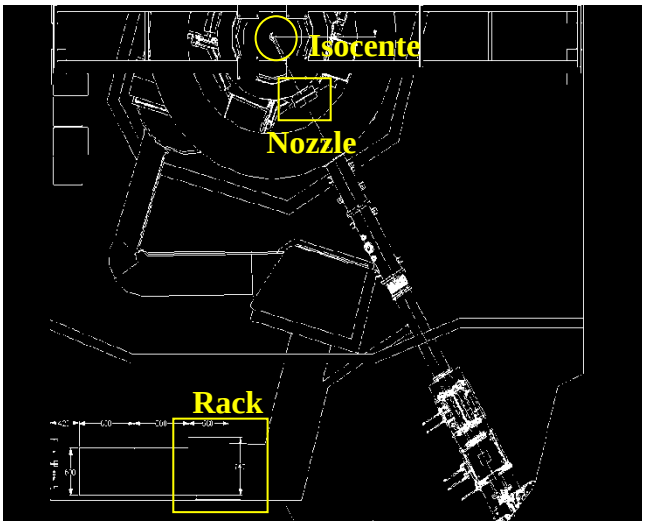

Figure 3. The beamline in the treatment room; the locations of the monitoring system and electronics rack are shown in the figure.

Neutrons arriving at the nozzle and the rack from backscattered radiation components, produced by the interaction between the primary carbon ion beam and patient's tissue. In the backward direction, there were only isotropic neutrons, resulting from nucleus evaporation; thus, a uniform neutron source in a solid angle [0, 2π] was assumed (positive *Z*-axis is the direction from the isocenter toward the hadron beamline).

2.3. Geometry of the location

The whole volum of the treatment room, interested by backscattered neutron radiation, was simulated as a parallelepiped of same dimensions (full of air).

2.4. Geometry of elements

The most important factor for setting up the geometry of irradiated elements is determining the shape and volume of sensitive elements. A meticulous study of the behavior of single elements depends on electronic devices; thus, no single choice can be made.

Firstly, precise dimensions of the nozzle (fig. 1) and the electronics rack (fig. 2) were set and described with respect to the isocenter, as shown in fig. 3. Then, geometric bodies available in FLUKA library were used to characterize the geometric shapes.

2.5. Materials

The nozzle was composed of two boxes (where the monitoring system was installed). It was divided into electronic parts (interface and read-out circuits) and the detector itself, which was situated in the beam direction; both parts were considered parallelepiped. The used material for the nozzle was aluminum with 5 cm thickness; the boxes were filled with air. In addition, the electronics rack, parallelepiped in shape, was made of iron (Fe).

2.6. Determination of neutron dose equivalent

In order to compare the obtained results with those of experimental studies in terms of the life performance of the device, we need to calculate neutron fluences impinging on devices (in our case, on the electronics rack and the surface of the nozzle). It must be stressed that neutron fluences are not the only interesting quantities to compute, since radiation monitoring detectors in the treatment room can provide an ambient dose equivalent or H*(10). It is useful to also evaluate H*(10) behavior in the same points, under the same irradiation conditions.

Here in the next section, definitions of major dose quantities are provided:

2.7. Effective dose coefficients:

Effective dose is defined as the sum of weighted equivalent doses in all tissues and organs of human body, as shown in equation (1):

$$E=\Sigma_T (H_T \times W_T) \quad (1)$$

Where H_T is the equivalent dose in tissue or organ T and W_T is the weighting factor for tissue T.

The equivalent dose H_T is calculated by:

$$H_T = \sum_R (w_R \times D_{T,R}) \quad (2)$$

Where $D_{T,R}$ is the average absorbed dose from radiation R in tissue T and W_R is the radiation weighting factor of radiation R, which depends on irradiation geometry.

Use of radiation weighting factor (W_R) was introduced by the International Commission on Radiological Protection (ICRP) to convert the absorbed dose (the real physical quantity) into a quantity which takes into account the effect of different radiations with different energies.

All radiation protection limits were expressed in effective dose. Since in practice, this quantity is not directly measurable, other quantities (operational quantities) were defined to give an approximation of the effective dose. One of the most widely equivalents used in experimental monitoring of radiation is ambient dose equivalent.

2.8. Ambient dose equivalent coefficients

The ambient dose equivalent H*(10) at the point of interest in the actual radiation field is the dose equivalent, which would be generated in the associated oriented and expanded radiation field at a depth of 10 mm along the radius of the Radiation Units and Measurements sphere (ICRU sphere, a sphere of 30 cm diameter, made of tissue equivalent material), oriented in the opposite direction of incident radiation [6].

2.9. Implementation in FLUKA

Both effective dose and ambient dose equivalent conversion coefficients were implemented in the FLUKA code and were enabled in the input file. Fluence-to-ambient dose equivalent conversion coefficients were based on ICRP74 values and those calculated by M. Pelliccioni. These conversions were implemented for protons, neutrons, charged pions, muons, photons, and electrons (conversion coefficients for other particles are approximated by these conversion coefficient). Fig. 4 shows the conversion coefficients, expressed in pSv·cm^2 in case of neutrons [6].

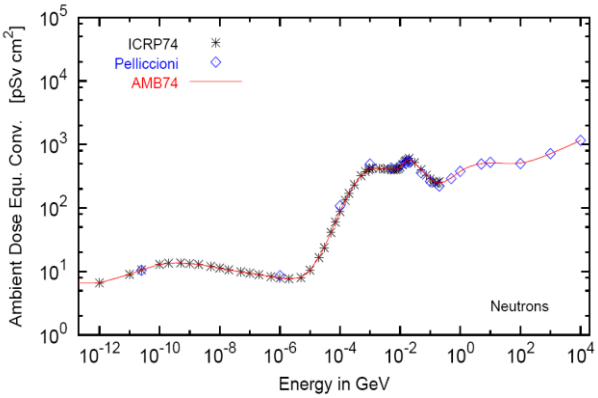

Figure 4. Fluence-to-ambient dose equivalent conversion coefficients for neutrons, as implemented in the FLUKA code.

3. Results

3.1. Spectra of secondary neutron

Fig. 5 shows the spectrum of neutrons produced by a 400 MeV/u carbon ion beam in the backward direction, while fig. 6 shows the comparison between this backward component and total energy spectrum (integrated over the whole solid angle). Total values obtained for neutron and proton yields in primary carbon ions and protons have been summarized in table 1.

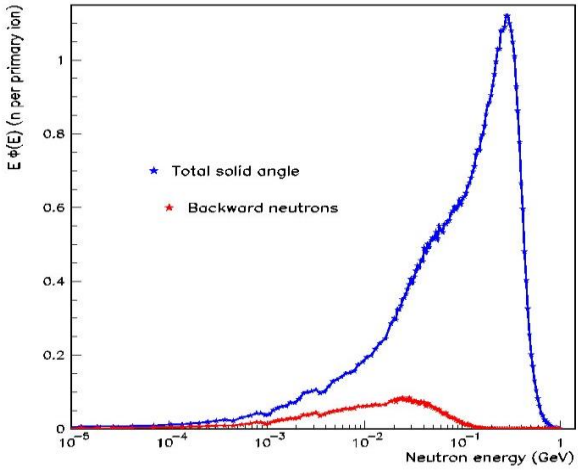

Figure 5. Spectrum of secondary neutrons produced in the backward direction by 400 MeV/u carbon ions, hitting a phantom made of ICRU tissue; a comparison is made with the total energy spectrum of secondary neutrons.

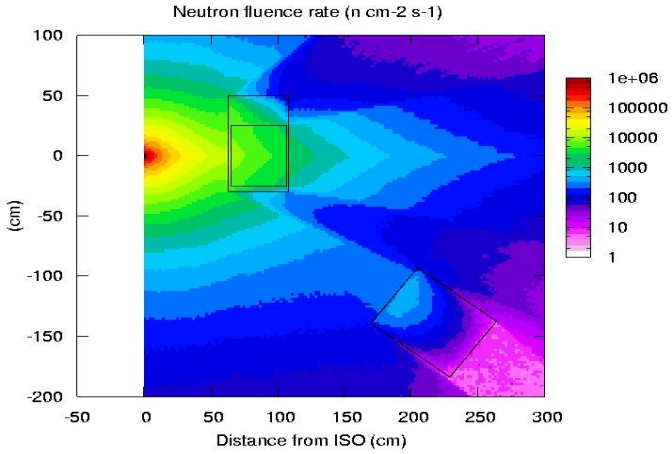

Figure 6. The fluence rate of secondary neutrons during treatment with 400 MeV/c carbon ions.

Table 1. Number of secondary neutrons and protons produced by carbon ion and proton beams on ICRU tissue

Target	Primary particles	n/primary	p/ primary
ICRU tissue	400 MeV/u ^{12}C ions	2.66	1.50
ICRU tissue	250 MeV protons	0.11	0.10

3.2. Neutron fluence and ambient dose equivalents

Figures 7 & 8 report the calculated quantities of neutron fluence and ambient dose equivalents, expressed in n/(cm^2.s) and µSv/s, respectively. The corresponding integrated values for a treatment period can be simply obtained by considering 132 s as the mean time of a typical treatment. The results were used to compute the life performance of electronic devices and sensors.

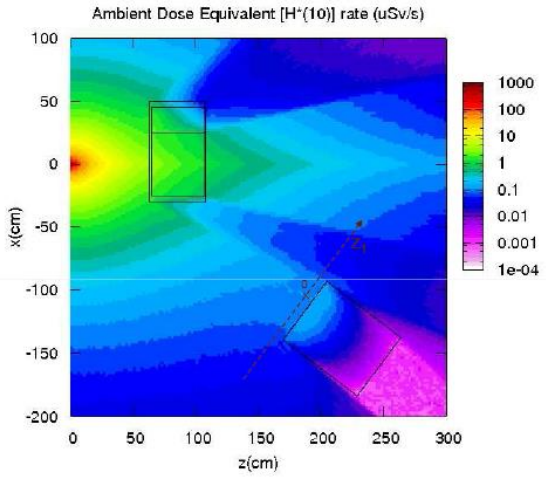

Figure 7. The ambient dose equivalent during treatment with 400 MeV/c carbon ions.

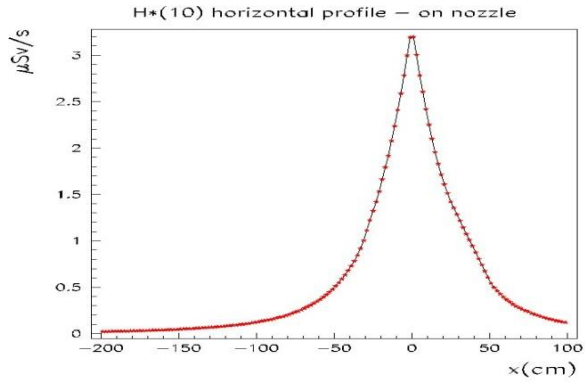

Figure 8. The irradiation profile at the nozzle entrance surface.

3.3. Dose profile

Fig. 9 presents the dose profile at the entrance surface of the nozzle, evaluated by the ambient dose equivalent (µSv/s versus distance in cm along the Z axis). Fig. 10 represents the dose profile at the entrance surface of the electronics rack, evaluated by the ambient dose equivalent (µSv/s versus cm).

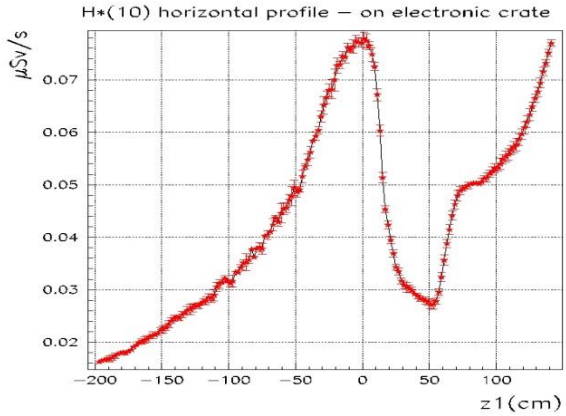

Figure 9. The irradiation profile at the electronics rack entrance along the *Z 1*-axis.

4. Discussion

4.1. Irradiation pattern

To evaluate the effect of radiation, neutron source intensity during the irradiation was characterized to integrate the results over a long operation time; the temporal length of one treatment is assumed to be 132 s, on average.

Number of neutrons per second during the irradiation is calculated by a higher intensity of ^{12}C beam (I_{ions}), multiplied by the yield (n_{back}) of backward neutrons:

$$I_{ions} \cdot n_{back} = (8 \cdot 10^8 / 2.2) \times 0.308 = 1.12 \cdot 10^8 \ n/s \qquad (3)$$

4.2. Spectra of secondary neutrons

So far, there have been no experimental data about neutron yields from 400 MeV/u carbon ions on body tissues. We used the results of

Monte Carlo study performed at CNAO, with the goal to offer a general reference for the yields of secondary particles in order to be applied in hadrontherapy[7].

In this study, interactions between accelerated carbon ions and protons on a phantom made of ICRU tissue (76.2% O, 11.1% C, 10.1% H, 2.6% N) (with a dimension of 30 x 30 x 30 cm^3) were simulated. Maximum operational energy for therapy was used for both proton and carbon ion beams. Secondary neutron and proton spectra were then fully characterized in a forward direction (0, 90°); only an input parameter for the backward radiation component was characterized (90°, 180°).

Fig. 4 shows the spectrum of secondary neutrons produced in the backward direction by 400 MeV/u carbon ions, hitting a phantom made of ICRU tissue. Fig. 5 shows the energy distribution of fig. 4, compared with the total energy spectrum of secondary neutrons.

In table 1, we can observe that secondary neutrons from primary carbon ions have the most critical value. For this secondary radiation, the portion of the yield related to the backscattered component (n_{back}) was evaluated:

$$n_{back} = 0.308 \text{ n/ion} \quad (4)$$

4.3. Neutron fluence and ambient dose equivalents

Neutron fluence rates, as well as ambient dose equivalents, were calculated in a modularspatial geometry, defined in the input file in a USRBIN card. Average of physical quantities was calculated for each volume. We used elementary volumes of 2 cm × 2 cm in the *XZ* plane (the plane represented in the figures), 55 cm high in the interval plane (-25 cm, +30 cm) in the vertical direction *y* (perpendicular to the beam). These dimensions were considered to cover the whole length of the nozzle box and the hot zone of the electronics rack.

4.4. Dose profiles

According to the results shown in fig. 8 for the behavior of ambient dose equivalent in the room, dose profiles at the entrance of the nozzle and electronics rack were evaluated. The profile in front of the nozzle (fig. 9) was calculated along the *X*-coordinate, which showed a clear peak dose at x=0. The profile in front of the rack was made along the Z_1 axis in fig. 10 and was centered at a peak dose around 0.08 µSv/s.

4.5. Assumptions

To evaluate the expected dose delivered to devices during a therapeutic treatment, occurs some assumptions as follows: treatment time, 3 min/h; working time, 12 h/day; 6 days/week; and annual working load, 52 weeks.

According to the simulation results, by using the maximum values of neutrons and radiation doses, was obtained the values of fluence rate, integrated fluence of neutrons, radiation dose and integrated radiation dose.

4.6. Experiments

In a study by Bourhaleb, the behavior of a VLSI chip for application as a front-end readout for a dosimeter or a monitor chamber in radiotherapy was evaluated. It was concluded that the electrical characteristics of the chip change by less than 1% for a total integrated neutron fluence of 4×10^{12}. Thus, the chip can be used over many years without any performance loss. Also, no single event upsets (SEUs) were observed up to a neutron fluence of 10^{14}. In addition, as experiments on LHC radiation damage indicated, neutron fluence effects can be studied in electronic technology (commercial electronics) and CMOS/non-CMOS (bipolar technology). CMOS technology is less sensitive to neutrons, compared to its bipolar counterpart. Generally, threshold values are approximately 10^{14} neutrons for CMOS and 10^{12} neutrons for non-CMOS. , [4].

5. Conclusion

A standard radiotherapy treatment delivers a fluence rate of secondary neutrons about 5×10^4 $(n\cdot cm^{-2})/s$ and 3.2 µSv/s on the nozzle. Thus, the nozzle will be exposed to an integrated neutron fluence of 3.4×10^{10} n/cm^2 and an integrated dose of about 2 Sv in a year and on

the electronic rack, delivers about 5×10^2 $(n\cdot cm^{-2})/s$ and 0.05 µSv/s. Thus, each year, the rack will be exposed to an integrated neutron fluence of 3.4×10^8 n/cm^2 and an integrated dose of about 34 mSv. Therefore, in comparison between experimental and FLUKA simulation results showed that the simulation value (as a threshold) is lower than the experimental threshold, which is responsible for less than 1% of changes of electrical characteristics, and would cause no SEU.

Acknowledgment

Thanks the medical physics group of experimental physics department of Torino University and all technical staff of workshop and laboratory of INFN of Torino. Thank a lot the CNAO administration for offering us the opportunity to study on this project.

References

1. A. Ansarinejad A, Attili A, Bourhaleb F, Cirio R, Donetti M, Garella MA, et al. The on-line detectors of the beam delivery system for Centro Nazionale di Adroterapia Oncologica (CNAO). Nuclear Physics B - Proceedings Supplements. 2009;197(1):185-9.
2. A. Ansarinejad, Development of online monitor detectors used for clinical routine in proton and ion therapy, Ph.D. Thesis, Torino, 2010 Nov, chapter 7.
3. Battistoni G, Muraro S, Sala PR, Cerutti F, Ferrari A, Roesler S, et al. The FLUKA code: description and benchmarking, Proceeding of the Hadronic Shower Simulation Workshop 2006, Fermilab 6-8; 2006 Sept, M. Albrow, R. Raja editors, AIP Conference Proceeding 896; 2007:31-49.
4. Fasso A, Ferrari A, Ranft J, Sala PR. FLUKA: a multi-particle transport code, CERN. 2005 Oct, INFN/TC_05/11, SLAC-R-773.
5. Pelliccioni M. Overview of fluence-to-effective dose and fluence-to-ambient dose equivalent conversion coefficients for high energy radiation calculated using the FLUKA code. Radiation Protection Dosimetry. 2000;88(4):279-97.
6. Ferrari A, Ferrarini M, Pelliccioni M. Secondary particle yields from 400 MeV/u carbon ion and 250 MeV proton beams incident on thick targets. Nuclear Instruments and Methods in Physics Research Section B: Beam Interactions with Materials and Atoms. 2011;269(13):1474-81.
7. Cirio R, Bourhaleb F, Degiorgis PG, Donetti M, Marchetto F, Marletti M, et al. Radiation damage studies of a recycling integrator VLSI chip for dosimetry and control of therapeutical beams. Nuclear Instruments and Methods in Physics Research Section A: Accelerators, Spectrometers, Detectors and Associated Equipment. 2002;482(3):752-60.